

## Higher-Order Stark Spectroscopy: Polarizability of Photosynthetic Pigments

Kaiqin Lao, Laura J. Moore, Huilin Zhou, and Steven G. Boxer\*

Department of Chemistry, Stanford University, Stanford, California 94305-5080

Received: October 14, 1994<sup>®</sup>

Stark spectra for nonoriented molecules with typical broad inhomogeneous line widths are obtained by applying an ac electric field and detecting the change in absorbance at the second harmonic of the field modulation frequency. The analysis of such data in terms of molecular parameters such as changes in dipole moment and polarizability is often difficult. We outline a new method, called higher-order Stark spectroscopy, in which the higher even-powered harmonics of the response to an ac field are measured. The method is applied to electronic states of photosynthetic pigments, including pure monomeric bacteriochlorophyll, the homo- and heterodimer special pair primary electron donors in photosynthetic reaction centers, and the carotenoid spheroidene, both pure in an organic matrix and in the B800–850 antenna complex. It is shown that even at a qualitative level these systems divide into two groups: those where the change in dipole moment dominates the change in polarizability (pure bacteriochlorophyll, the heterodimer, and spheroidene in the antenna complex) and those where the polarizability dominates the change in dipole moment (pure spheroidene and the homodimer special pair).

A quantitative analysis of the Stark effect spectrum provides information on molecular properties associated with the movement of charge such as the change in dipole moment ( $\Delta\mu$ ), polarizability ( $\Delta\alpha$ ), and hyperpolarizability for an electronic<sup>1</sup> or vibrational<sup>2</sup> transition. For a uniaxially oriented system, the contributions from  $\Delta\mu$  and  $\Delta\alpha$  can be readily distinguished as the former depends linearly on the field, while the latter depends quadratically on the field. However, for isotropic, immobilized samples (frozen glasses or polymer films), which are far easier to study and are often the only conditions under which samples can be studied, the contributions from  $\Delta\mu$  and  $\Delta\alpha$ , as well as all other electrooptic parameters, depend on the same power of the field; consequently, the contributions can only be obtained by analyzing the Stark line shape. In the following we outline a new experimental method, called higher-order Stark spectroscopy, for obtaining more information than was previously possible about the electrooptic properties of molecules. We specifically apply this method to several photosynthetic pigments. By comparing the higher-order Stark spectra for several different types of chromophores in different environments, it is possible, even at a qualitative level, to obtain information on the relative contributions of  $\Delta\mu$  and  $\Delta\alpha$ . We find directly that the first electronic excited state of the special pair primary electron donor P in photosynthetic reaction centers (RCs) has a very large polarizability, a conclusion which was previously suggested from conventional low-temperature Stark spectroscopy via a complex line shape analysis.<sup>3</sup> In a subsequent paper, we will show that a quantitative analysis of the higher-order Stark spectra can be used to obtain the diagonal elements of the polarizability tensor of P, and this information can be used to obtain the magnitude and direction of a large and highly anisotropic matrix electric field in the vicinity of P.<sup>4</sup>

The highest-sensitivity conventional measurements of the Stark effect for nonoriented systems are usually made by application of an ac electric field with detection of the change in absorption at the second harmonic  $2\omega$  of the field modulation frequency  $\omega$  using lock-in detection.<sup>5</sup> For a nonoriented, immobilized system, the resulting change in absorption  $\Delta A(\nu, F^2)$  as a function of probe wavenumber  $\nu$  measured at the second

harmonic of the field modulation frequency is a sum of the zeroth, first, and second derivatives of the absorption spectrum.<sup>6</sup> The zeroth-derivative component is usually small and is associated with the polarizability (**A**) and hyperpolarizability (**B**) tensors of the transition dipole moment. The second-derivative component depends exclusively on the difference dipole moment between the electronic excited and ground states ( $\Delta\mu$ ) and the angle  $\zeta_A$  between  $\Delta\mu$  and the transition dipole moment direction (**p**) used to probe the Stark effect. The first-derivative component reflects contributions from the change of the polarizability,  $\Delta\alpha$ , as well as contributions from the **A** tensor. Because cross terms between  $\Delta\mu$  and **A** can also contribute significantly to the first-derivative component, it is often not possible to reliably extract information on  $\Delta\alpha$  from the conventional Stark spectra. The polarizability tensor  $\Delta\alpha$  is especially useful in complex, organized systems because it determines both the magnitude and anisotropy of the sensitivity of the probe chromophore to electrostatic interactions with its environment. This is manifested as an induced dipole moment,  $\Delta\mu_{\text{ind}}$ , due to the interaction between the matrix field of the environment,  $\mathbf{F}_{\text{matrix}}$ , and  $\Delta\alpha$ . As illustrated in the following, even at a qualitative level, higher-order Stark spectroscopy can provide some information about  $\Delta\alpha$ .

The field-induced change  $\Delta A$  in absorbance by an externally applied sinusoidal electric field  $\mathbf{F}(\omega) = \mathbf{F}_0 \sin(\omega t)$  is given by

$$\Delta A(\nu, \mathbf{F}) = \Delta A(\nu, \mathbf{F}^2, 2\omega) + \Delta A(\nu, \mathbf{F}^4, 4\omega) + \Delta A(\nu, \mathbf{F}^6, 6\omega) + \dots \quad (1)$$

Changes in absorbance,  $\Delta A(\nu, \mathbf{F}^2, 2\omega)$ ,  $\Delta A(\nu, \mathbf{F}^4, 4\omega)$ ,  $\Delta A(\nu, \mathbf{F}^6, 6\omega)$ , etc., are recorded using lock-in detection at the second-, fourth-, and sixth-harmonic frequencies, respectively, of the field modulation frequency  $\omega$ . The  $n$ th-order spectrum depends on the  $n$ th power of the applied field,  $\mathbf{F}^n$ . Like the conventional or  $2\omega$  Stark effect, the higher-order Stark spectra can be fit to sums of derivatives of the absorption line shape. For example, in the case of the  $4\omega$  spectrum,  $\Delta A(\nu, \mathbf{F}^4, 4\omega)$  is fit to the sum of up to the fourth derivative of the absorption line shape. Additionally, for each  $n$ th-order Stark spectrum, the  $n$ th-derivative component depends only upon  $\Delta\mu$  and  $\zeta_A$ . Thus, if the  $n$ th-order Stark spectrum is dominated by the  $n$ th derivative

<sup>®</sup> Abstract published in *Advance ACS Abstracts*, December 15, 1994.

of the absorption spectrum, it is immediately evident that  $\Delta\mu$  dominates  $\Delta A(\nu, F)$ . An even simpler diagnostic for this case is that the  $(n + 2)$ -order Stark spectrum is the second derivatives of the  $n$ th-order spectrum. As seen below, this simple diagnostic is quite powerful because it is possible to obtain Stark spectra with good signal to noise, whereas it is quite difficult to obtain good-quality higher derivatives of the absorption spectrum.

### Experimental Methods

Implementation of this new method is made possible by three technical advances. First, it is now possible to apply very large electric fields to samples, including frozen aqueous samples. The key is to work with very thin samples, typically 10–30  $\mu\text{m}$ . High fields are critical because the  $n$ th-order contribution to the Stark effect depends on the  $n$ th power of the applied electric field strength (eq 1). Even at the highest applied electric fields, the higher-order contributions to the Stark effect are much smaller than the second-order (conventional) contribution. Second, several manufacturers have recently developed digital lock-in amplifiers with exceptional dynamic reserve, so that even a small signal coming from the higher-order harmonics is detectable. Third, it is essential that the frequency of the applied electric field be as free as possible of harmonic distortion because combinations of components other than the desired  $n$ th harmonic will contaminate the signal  $n$ th harmonic signal [e.g.,  $(\cos \omega t)(\cos 3\omega t)$  gives a  $\cos 4\omega t$  component]. This problem is currently minimized by using a low-distortion, digitally synthesized sine wave from the lock-in amplifier to generate the sine wave in the power supply. Some harmonic distortion remains, and this is currently the main limitation in obtaining signals at higher order than the eighth harmonic.

Aside from these developments, the methodology is similar to that used for obtaining conventional Stark effect data.<sup>5</sup> All spectra were obtained in normal incidence. For  $2\omega$ ,  $4\omega$ , and  $6\omega$  spectra,  $\Delta A = (2\sqrt{2}/2.303)\Delta I/I$ ,  $(8\sqrt{2}/2.303)\Delta I/I$ , and  $(32\sqrt{2}/2.303)\Delta I/I$ , respectively, where  $\Delta I/I$  is the signal from the lock-in amplifier. This converts the signal to what would be observed if a dc field of  $|F|$  were applied. The difference in the conversion factors for different harmonics arises from the fact that 1/2 of a dc signal is obtained by lock-in detection at  $2\omega$ , 1/8 at  $4\omega$ , and 1/32 at  $6\omega$ . The sample of interest is introduced into a sample cell made of glass or quartz slides which are coated with a semitransparent electrode (indium tin oxide) and separated by inert spacers. The sample is immersed in liquid nitrogen, and the change in transmission is probed with light passed through a high-resolution monochromator (needed because higher-order Stark spectra often exhibit high-resolution structure, see below) and detected with a Si photodiode.

Bacteriochlorophyll *a* (BChl *a*) was isolated by standard methods<sup>7</sup> from *Rb. sphaeroides* cells and was dissolved in toluene with pyridine (100:1, v/v). *Rb. sphaeroides* wild-type cells were grown in the light; the heterodimer strain (M)H202L was prepared by site-directed mutagenesis using a deletion strain kindly provided by Joanne Williams, and cells were grown semiaerobically in the dark. RCs were obtained by standard procedures.<sup>8</sup> The B800–850 antenna complex was isolated from *Rb. sphaeroides* cells grown anaerobically in the light as described in ref 9. Under these conditions essentially all of the carotenoid is spheroidene.<sup>10</sup> All measurements on the proteins were done on 1:1 (v/v) glycerol/buffer (10 mM Tris, pH 8.0, 0.01% LDAO) samples. Pure spheroidene was isolated from whole cells grown photosynthetically as described in ref 10 and was dissolved in toluene.

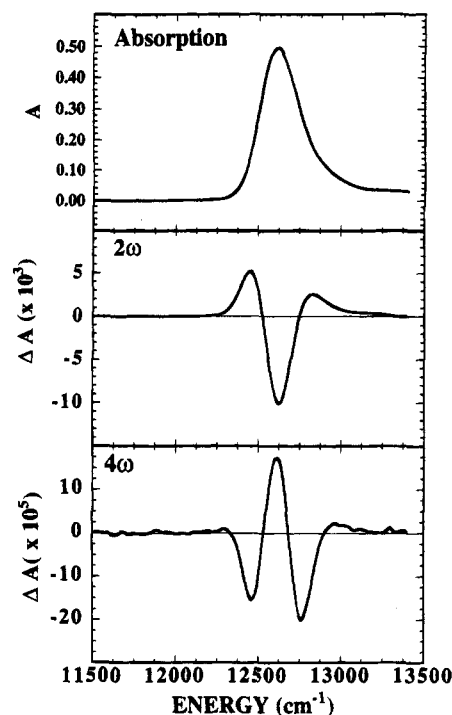


**Figure 1.** Absorption,  $2\omega$ , and  $4\omega$  Stark spectra of the  $Q_y$  band of monomeric bacteriochlorophyll *a* in toluene/pyridine (100:1 v/v) at 77 K. The spectra were taken at fields of 0.89 and 0.96 MV/cm for  $2\omega$  and  $4\omega$ , respectively, and then scaled to a field of 1 MV/cm for comparison.

### Results and Discussion

**Pure Bacteriochlorophyll *a*.** Figure 1 shows the absorption, conventional ( $2\omega$ ), and  $4\omega$  Stark spectra of pure monomeric BChl *a*. It is apparent that the  $4\omega$  spectrum can be obtained with excellent signal to noise and that its line shape is dominated by the fourth derivative of the absorption spectrum. This is confirmed by comparing the numerical second derivative of the  $2\omega$  signal with the  $4\omega$  Stark signal as shown in Figure 2. It is seen that the central minimum of the  $2\omega$  and maximum of the  $4\omega$  Stark spectra are at nearly the same wavelength as the absorption maximum, demonstrating that there is little spectral shift (i.e., first-derivative contribution) upon application of the electric field. This is an example of a situation in which  $\Delta\mu$  completely dominates  $\Delta\alpha$ .  $\Delta\alpha$  for BChl *a* is on the order of 10–50  $\text{\AA}^3$ ,<sup>11</sup> whereas  $\Delta\mu$  is approximately 2 D.<sup>12</sup> Essentially identical results are obtained for pure, monomeric bacteriopheophytin *a* (data not shown).

**Reaction Centers.** Figure 3 shows the absorption and Stark spectra for wild-type RCs in the  $Q_y$  region. We focus here on the dramatic difference between the Stark spectrum of the special pair primary electron donor P, a dimer of BChls, and isolated, pure BChl *a* (cf. Figure 1). The  $2\omega$  Stark spectrum at 77 K is difficult to analyze: it resembles the second derivative of the absorption, but closer inspection and line shape analysis at 1.5 K indicate a substantial first-derivative contribution.<sup>3</sup> The  $4\omega$  spectrum does not resemble the fourth derivative of the absorption; rather, it has a shifted and distorted second-derivative line shape. Thus, it is immediately clear that the electrooptic behavior of the special pair is very different from a monomeric BChl *a*. Examination of the monomer region of the RC higher-order Stark spectra shows that the monomeric BChls (denoted B) and monomeric bacteriopheophytins (BPheo, denoted H) have approximately second- and fourth-derivative line shapes in the  $2\omega$  and  $4\omega$  spectra, respectively, consistent with the properties of the isolated monomers.

The contrast between monomeric BChl and the dimeric

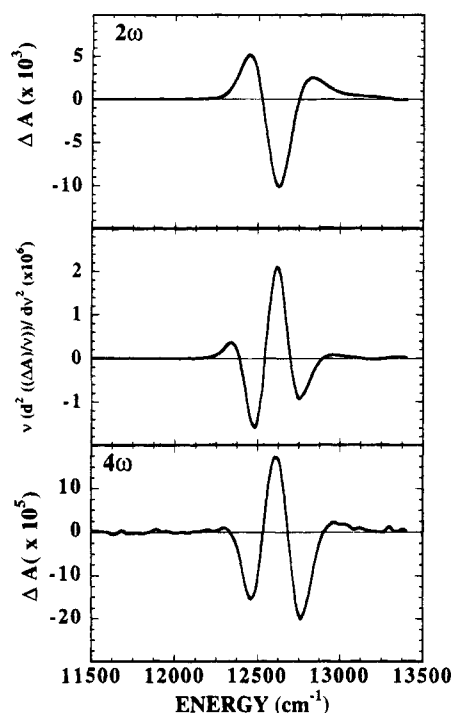


**Figure 2.** Comparison of the  $2\omega$  Stark (top panel), its numerical second derivative (middle panel), and the  $4\omega$  Stark spectrum (lower panel) of bacteriochlorophyll *a* showing that the  $4\omega$  spectrum is essentially the second derivative of the  $2\omega$  signal, the latter being essentially the second derivative of the absorption spectrum. The Stark spectra are taken from Figure 1.

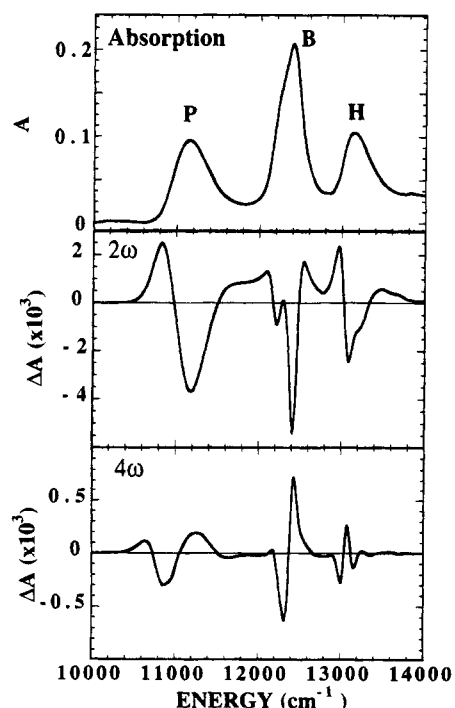


**Figure 3.** Absorption,  $2\omega$ , and  $4\omega$  Stark spectra of wild-type *Rb. sphaeroides* reaction centers in the  $Q_y$  region at 77 K in a glycerol/buffer glass ( $|F| = 1.07$  MV/cm).

special pair in RCs can be further accentuated by comparing the heterodimer special pair [(M)H202L], in which one of the BChls comprising P is converted to a BPhe,<sup>13</sup> with the homodimer in wild type. As shown in Figure 4, the absorption of the heterodimer is spread out, with evidence for two absorption bands.<sup>14</sup> A substantial  $2\omega$  Stark effect is seen for the lower-energy feature; however, it is quite difficult to perform a quantitative analysis because the absorption, from which

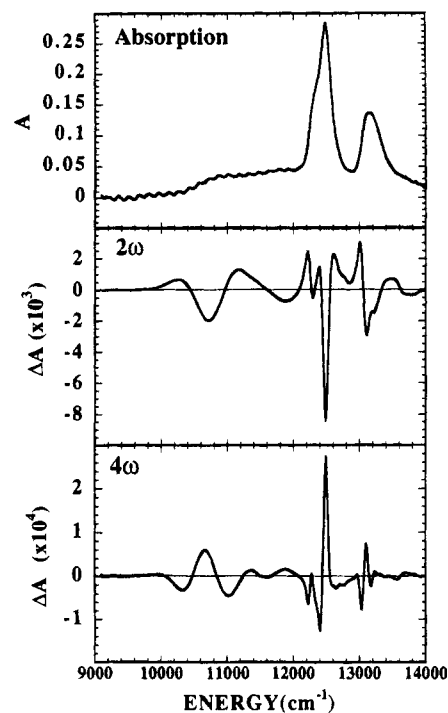


**Figure 4.** Absorption,  $2\omega$ , and  $4\omega$  Stark spectra of the heterodimer mutant, (M)H202L, reaction center of *Rb. sphaeroides* at 77 K in a glycerol/buffer glass ( $|F| = 0.89$  MV/cm). Interference fringes are present in the absorption spectrum.<sup>15</sup>

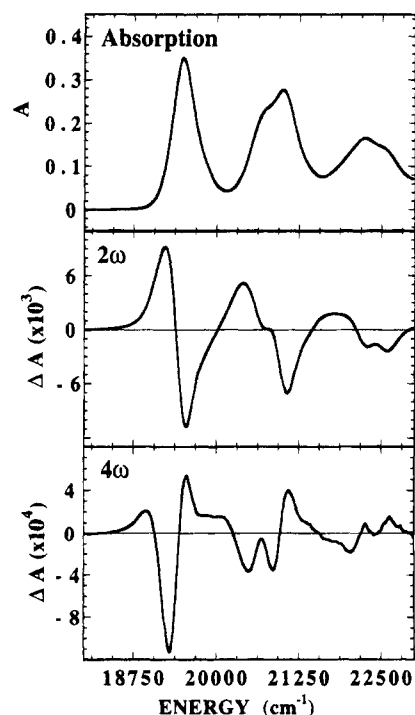


**Figure 5.** Absorption,  $2\omega$ , and  $4\omega$  Stark spectra of pure spheroidene at 77 K in a toluene glass ( $|F| = 0.97$  MV/cm).

derivatives are obtained, is so poorly defined.<sup>15</sup> The  $4\omega$  Stark spectrum of this feature is very large and is nearly exactly the second derivative of the  $2\omega$  signal. Thus, for this absorption feature of the heterodimer special pair,  $\Delta\mu$  completely dominates, in striking contrast to the native homodimer.

**Carotenoids.** It is instructive to examine the higher-order Stark spectra of conjugated polyenes. They are very interesting in their own right, and they provide a useful comparison with the BChl-containing species described above because it is well established that isolated polyenes have a large excited state polarizability. Figure 5 shows the absorption and Stark spectra

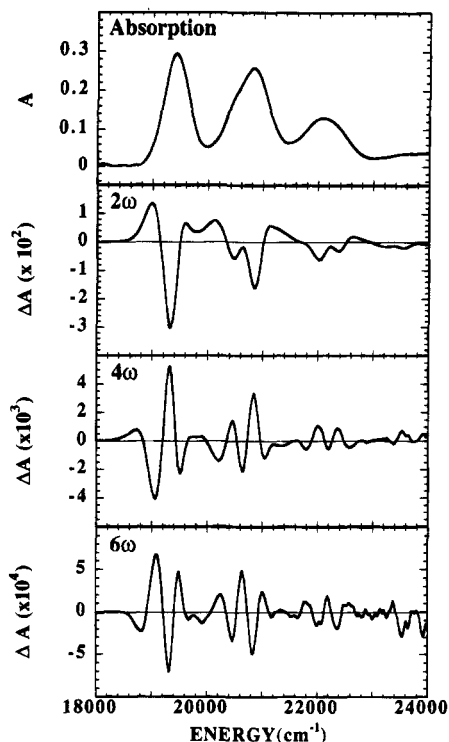


**Figure 6.** Absorption,  $2\omega$ ,  $4\omega$ , and  $6\omega$  Stark spectra of the carotenoid (spheroidene) region of the B800–850 antenna complex of *Rb. sphaeroides* grown anaerobically at 77 K in a glycerol/buffer glass ( $|F| = 0.92$  MV/cm).

for pure spheroidene in frozen toluene. The conventional ( $2\omega$ ) Stark spectrum has a substantial first-derivative contribution,<sup>16</sup> consistent with the known large polarizabilities of conjugated polyenes.<sup>17,18</sup> It is further seen that the  $4\omega$  and higher-order Stark spectra line shapes are not the second and higher derivatives of the  $2\omega$  spectrum. Interestingly, they resemble the line shapes of the homodimer P in wild-type RCs. In photosynthetic membranes, spheroidene is bound to both the antenna and RC complexes. Figure 6 shows the Stark spectrum of spheroidene in the B800–850 antenna complex. We had shown earlier that in this complex, in striking contrast to the isolated polyene, spheroidene exhibits an extremely large dipole moment, presumably induced by the organized electrostatic environment interacting with the large polarizability of the polyene.<sup>16</sup> The signature of this behavior is that the  $2\omega$  Stark spectrum is dominated by the second derivative of the absorption line shape, the  $4\omega$  Stark spectrum is approximately the second derivative of the  $2\omega$  spectrum, and the  $6\omega$  spectrum is approximately the second derivative of the  $4\omega$  spectrum. Figure 7 shows the electric field dependence of the higher-order Stark signal intensity, demonstrating the expected  $n$ th-power dependence on electric field for the  $n$ th-order Stark spectrum. Similar field dependence data were collected for all species examined up to the highest order studied. We were only able to obtain high signal-to-noise spectra to such high order for spheroidene in the B800–850 complex, because of the huge value of  $\Delta\mu$ , so only this data is shown.

From the spectra shown in Figures 1–7, it is evident that high signal-to-noise higher-order Stark data can be obtained, even under the otherwise unfavorable circumstances of frozen aqueous glasses and biological materials. A detailed analysis of the line shapes of these spectra can provide quantitative information on many electrooptic parameters of these chromophores, and such an analysis is in progress;<sup>4</sup> however, we restrict our attention in this Letter to several clear qualitative conclusions. It is observed that at all orders the chromophores cluster

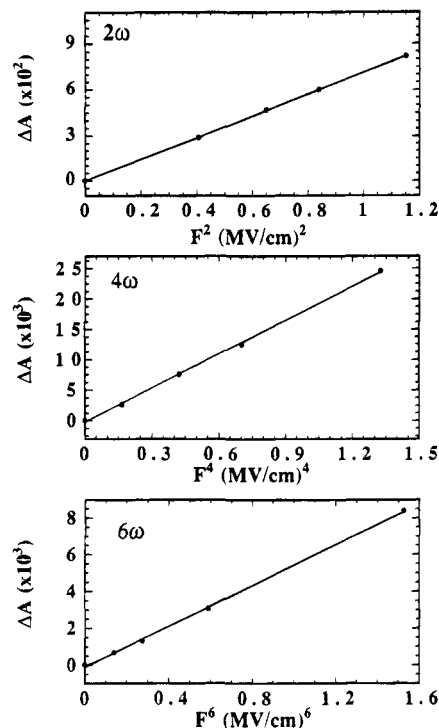


**Figure 7.** Dependence of the amplitude of the Stark signal on the applied electric field for the  $2\omega$ ,  $4\omega$ , and  $6\omega$  Stark spectra of spheroidene in B800–850 (see Figure 6).

into two groups: monomeric BChl *a*, the heterodimer special pair in the RC, and spheroidene in the B800–850 complex have Stark spectra with similar second, fourth, etc., derivative line shapes,<sup>19</sup> while the homodimer in wild-type RCs and pure spheroidene in a nonpolar organic glass also have similar line shapes. Although those may seem like odd chromophores to compare, it is very useful because it is well-known that pure polyenes have large excited state polarizabilities and relatively small (or negligible) changes in dipole moment, whereas cyclic aromatics, like BChl *a*, have relatively small excited state polarizabilities. Thus, without needing a complex line shape analysis,<sup>3,15</sup> it is evident that homodimer P has a large excited state polarizability and that the heterodimer special pair has a large excited state dipole moment. The role of intradimer charge-transfer states in producing this effect has been discussed elsewhere.<sup>3,14,15,20</sup> Unfortunately, it is not possible to extract the special pair out of the RC and measure its intrinsic  $\Delta\mu$ , as is possible for spheroidene. If we assert that the intrinsic  $\Delta\mu$  of the special pair is very small and that the observed  $\Delta\mu$  is induced by the matrix electric field, then, as discussed in detail in ref 3, we are led to conclude that the matrix electric field in the vicinity of P is large and highly anisotropic, and this may have significant functional consequences. At this time the Stark effect line shape for the homodimer special pair in the RC is still not well understood. Measurements are in progress at 1.5 K where there is considerable structure in the absorption and higher-order Stark spectra which may provide further insight into the excited state which initiates photosynthesis.

**Acknowledgment.** This work was supported in part by a grant from the NSF Biophysics Program.

#### References and Notes

- (1) Liptay, W. In *Excited States*; Lim, E. C., Ed.; Academic Press: New York, 1974; Vol. 1, pp 129–229.
- (2) Chattopadhyay, A.; Boxer, S. G. *J. Am. Chem. Soc.*, submitted.
- (3) Middendorf, T. R.; Mazzola, L. T.; Lao, K.; Steffen, M. A.; Boxer, S. G. *Biochim. Biophys. Acta* **1993**, *1143*, 223.

- (4) Lao, K.; Zhou, H.; Moore, L. J.; Boxer, S. G., to be published.
- (5) Boxer, S. G. In *The Photosynthetic Reaction Center*; Diesenhofer, J., Norris, J. R., Eds.; Academic Press: London, 1993; Vol. II, pp 179–220.
- (6) This applies for an isolated (nonoverlapping) absorption band where the electro-optic parameters are constant across the inhomogeneous band. The latter may not always be the case, especially when  $\Delta\mu$  is induced by a matrix field. See, e.g.; Vauthey, E.; Voss, J.; de Caro, C.; Renn, A.; Wild, U. P. *Chem. Phys.* **1994**, *184*, 347–356. This may be a significant factor for the special pair.<sup>3</sup> The higher-derivative nature of the higher-order Stark spectra may prove useful in analytical applications, when many overlapping bands are present.
- (7) Scherz, A.; Parson, W. W. *Biochim. Biophys. Acta* **1984**, *766*, 653.
- (8) Paddock, M. L.; Rongey, S. H.; Abresch, E. C.; Feher, G.; Okamura, M. Y. *Photosynth. Res.* **1988**, *17*, 75–91.
- (9) Gottfried, D. S.; Stocker, J. W.; Boxer, S. G. *Biochim. Biophys. Acta* **1991**, *1059*, 63–75.
- (10) Cogdell, R. J.; Parson, W. W.; Kerr, M. J. *Biochim. Biophys. Acta* **1976**, *430*, 83.
- (11) Renge, I. *Chem. Phys.* **1992**, *167*, 173–184. Krawczyk, S. *Biochim. Biophys. Acta* **1991**, *1056*, 64–70. Davidsson, A. *Chem. Phys.* **1980**, *45*, 409–414.
- (12) Lockhart, D.; Boxer, S. *Proc. Natl. Acad. Sci. U.S.A.* **1988**, *85*, 107–111.
- (13) Bylina, E. J.; Youvan, D. C. *Proc. Natl. Acad. Sci. U.S.A.* **1988**, *85*, 7226–7230. Kirmaier, C.; Holten, D.; Bylina, E.; Youvan, D. C. *Proc. Natl. Acad. Sci. U.S.A.* **1988**, *85*, 7562–7566.
- (14) DiMagno, T. J.; Bylina, E. J.; Angerhofer, A.; Youvan, D. C.; Norris, J. *Biochemistry* **1990**, *29*, 899–907. Hammes, S. L.; Mazzola, L.; Boxer, S. G.; Gaul, D. F.; Schenck, C. C. *Proc. Natl. Acad. Sci. U.S.A.* **1990**, *87*, 5682.
- (15) The oscillatory structure superimposed on the absorption is due to interference fringes for this very thin sample. These fringes are extremely useful because they permit a precise calibration of the sample thickness at low temperature, one of the largest sources of experimental error in these measurements. On the other hand, it is obviously not possible to take derivatives of the absorption spectrum when fringes are present, so separate samples which are thicker or whose thickness is slightly less homogeneous (the typical case) must be used to obtain derivatives. This can be a problem because the precise line shape is so important. Of course, the fringes are absent in the field-modulated spectra.
- (16) Gottfried, D. S.; Steffen, M. A.; Boxer, S. G. *Science* **1991**, *251*, 662–65. Gottfried, D. S.; Steffen, M. A.; Boxer, S. G. *Biochim. Biophys. Acta* **1991**, *1059*, 76–90.
- (17) Liptay, W.; Wortmann, R.; Böhm, R.; Detzer, N. *Chem. Phys.* **1988**, *120*, 439–444.
- (18) Ponder, M.; Mathies, R. *J. Phys. Chem.* **1983**, *87*, 5090–5098.
- (19) The magnitudes of the change in absorption are vastly different because the magnitudes of  $\Delta\mu$  are very different for these different chromophores.
- (20) Lathrop, E. J. P.; Friesner, R. A. *J. Phys. Chem.* **1994**, *98*, 3056–66.

JP9427746